

The lepton flavor violating signal of the charged scalar ϕ^\pm and $\phi^{\pm\pm}$ in photon-photon collision at the ILC

Guo-Li Liu^{1,3}, Fei Wang^{1,3}, Qing-Guo Zeng^{2,4}

¹ *Physics Department, Zhengzhou University, Henan, 450001, China*

² *Department of Physics, Shangqiu Normal University, Shangqiu 476000, China*

³ *Kavli Institute for Theoretical Physics,*

Academia Sinica, Beijing 100190, China

⁴ *Department of Physics, Liaoning Normal University, Dalian 116029, China*

The hitherto unconstrained lepton flavor mixing, induced by the new charged scalar ϕ^\pm and $\phi^{\pm\pm}$ predicted by many new physics models such as Higgs triplet models, may lead to the lepton flavor violating productions of $\tau\bar{\mu}$, $\tau\bar{e}$ and $\mu\bar{e}$ in photon-photon collision at the proposed international linear collider (ILC).

In this paper, we consider the contributions of the ϕ^\pm and $\phi^{\pm\pm}$ in the context of the Higgs triplet models to the processes $\gamma\gamma \rightarrow l_i\bar{l}_j$ ($i, j = e, \mu, \tau, i \neq j$) and find that they can be good channels to probe these new physics models. The lepton flavor violating processes $\gamma\gamma \rightarrow l_i\bar{l}_j$ ($i, j = e, \mu, \tau, i \neq j$) occur at a high rate due to the large mixing angle and the large flavor changing coupling, so, in view of the low standard model backgrounds, they may reach the detectable level of the ILC for a large part of the parameter space. Since the rates predicted by the standard model are far below the detectable level, these processes may serve as a sensitive probe for such new physics models.

Keywords: new charged scalar ϕ^\pm and $\phi^{\pm\pm}$, lepton flavor violating processes, photon-photon collision, Higgs triplet model

PACS numbers: 13.85.Lg, 13.66.De, 12.60.Fr, 13.66.-a

I. INTRODUCTION

Lepton flavor violating (LFV) interactions are missing in the Standard Model (SM), so any observation of the LFV processes would serve as a robust evidence for new physics beyond the SM.

Many kinds of models beyond the SM, such as the Higgs triplet models (HTM) [1, 2] predict the presence of charged scalars ϕ^\pm and $\phi^{\pm\pm}$. Such triplet Higgs fields can induce LFV processes at the proposed international linear collider (ILC)[3], such as the productions of $\tau\bar{\mu}$, $\tau\bar{e}$ and $\mu\bar{e}$ via e^+e^- , $e^-\gamma$ and $\gamma\gamma$ collisions. It is noticeable that the productions of $\tau\bar{\mu}$, $\tau\bar{e}$ and $\mu\bar{e}$ in $\gamma\gamma$ collision have not been studied in this scenario. It is also noticeable that all these LFV processes at the ILC involve the same part of the parameter space of such new physics models. Therefore, it is necessary to compare all these processes to find out which process is the best to probe these models.

Due to its rather clean environment, the ILC will be an ideal machine to probe new physics. The LIC is a proposed future e^+e^- collider, designed to fill e^+e^- collisions at energies from 0.5 to 1 TeV, with the possibility to update to 3 TeV, which is actually designed to be compact linear collider(CILC)[4].

In addition to e^+e^- collision, we can also realize $\gamma\gamma$ collision[5] in such a collider with the photon beams generated by the backward Compton scattering of incident electron- and laser-beams.

The LFV productions in $\gamma\gamma$ collision may be more important than those in e^+e^- collision. Firstly, $e^+e^- \rightarrow \ell_i\bar{\ell}_j$ can be generated by means of the photon s-channel like $e^+e^- \rightarrow \gamma^* \rightarrow \ell_i\bar{\ell}_j$, with $S^{\pm\pm}$ and/or H^\pm running inside the loop, which is at the same order as cross section of the $\gamma\gamma \rightarrow \ell_i\bar{\ell}_j$. However, the e^+e^- production is expected to be sub-dominant with respect to the production from $\gamma\gamma$ collision since the latter gets the usual logarithmic enhancements induced by the phase space integration of the u - and t -channels. More importantly, compared with the collision in the e^+e^- , the lepton flavor violating productions at the $\gamma\gamma$ collision are essentially free of any SM irreducible background. So the LFV productions in the $\gamma\gamma$ collision are a good probe for new physics models.

In this work, we will study the LFV processes $\gamma\gamma \rightarrow \ell_i\bar{\ell}_j$ ($\ell_i = e, \mu, \tau$ and $i \neq j$) which is induced by the new charged scalars ϕ^\pm and $\phi^{\pm\pm}$ in HTM models. We calculate the production rates to figure out if they can reach the sensitivity of the photon-photon collision

of the ILC within the allowed parameter space of this scenario.

The work is organized as follows. We will briefly discuss the HTM models in Section II and III, giving the involved new couplings and the parameters in our calculation. In Section IV we give the calculation results in the HTM models and compare them with other models, such as the supersymmetry, the little Higgs and technicolor models. Section V is our conclusion.

II. THE HIGGS TRIPLET MODELS AND THE RELEVANT COUPLINGS

Many new physics scenarios predict new particles which lead to significant LFV signals. For example, the charged scalars ϕ^\pm and $\phi^{\pm\pm}$, which are predicted by various specific models beyond the SM, can lead to the large tree-level lepton flavor changing couplings. Such couplings can have significant contributions to the realization of some LFV processes.

In the Higgs triplet model (HTM) [1, 2] an extra $SU(2)_L$ isospin scalar triplet is added to the SM state spectrum. The neutrinos can directly obtain a majorana mass from the triplet through the gauge invariant Yukawa interaction, in the absence of the right-handed neutrinos. The Yukawa interactions can be written as [6]:

$$\mathcal{L} = h_{ij}\psi_{iL}^T C i\tau_2 \Delta \psi_{jL} + h.c. , \quad (1)$$

where the coupling $h_{ij}(i, j = 1, 2, 3)$ is complex and symmetric. C and τ_2 denote the Dirac charge conjugation operator and the second Pauli matrix, respectively. $\psi_{iL} = (\nu_i, l_i)_L^T$ is the left-handed lepton doublet. Δ is a new complex triplet fields of $Y = 2$ with a 2×2 representation:

$$\Delta = \begin{pmatrix} \Delta^+/\sqrt{2} & \Delta^{++} \\ \Delta^0 & -\Delta^+/\sqrt{2} \end{pmatrix} \quad (2)$$

The non-zero vacuum expectation value (VEV) $\langle \Delta^0 \rangle$ of the triplet fields Δ , results in the following neutrino mass matrix:

$$m_{ij} = 2h_{ij}\langle \Delta^0 \rangle = \sqrt{2}h_{ij}v_\Delta \quad (3)$$

The necessary non-zero v_Δ is generated by the minimization of the most general $SU(2) \otimes U(1)_Y$ invariant Higgs potential, which can be written as follows [7, 8] (with $\Phi = (\phi^+, \phi^0)^T$):

$$V = m^2(\Phi^\dagger \Phi) + \lambda_1(\Phi^\dagger \Phi)^2 + M^2\text{Tr}(\Delta^\dagger \Delta) + \lambda_2[\text{Tr}(\Delta^\dagger \Delta)]^2 + \lambda_3\text{Det}(\Delta^\dagger \Delta)$$

$$+\lambda_4(\Phi^\dagger\Phi)\text{Tr}(\Delta^\dagger\Delta)+\lambda_5(\Phi^\dagger\tau_i\Phi)\text{Tr}(\Delta^\dagger\tau_i\Delta)+\left(\frac{1}{\sqrt{2}}\mu(\Phi^T i\tau_2\Delta^\dagger\Phi)+h.c\right) \quad (4)$$

For small v_Δ/v , the expression for v_Δ resulting from the minimization of V is:

$$v_\Delta \simeq \frac{\mu v^2}{2M^2 + (\lambda_4 + \lambda_5)v^2} . \quad (5)$$

The possibility of the observations of various lepton flavor violating processes induced by the triplet Higgs bosons can provide a probe for the neutrino masses and mixing through the relation (3), and thus a direct test of the model.

In the HTM models, there are seven Higgs bosons ($H^{++}, H^{--}, H^+, H^-, H^0, A^0, h^0$) [6]. The doubly charged $H^{\pm\pm}$ can be identified with a component of the triplet scalar field $\Delta^{\pm\pm}$. The remaining eigenstates H^\pm, H^0, A^0, h^0 are the mixtures of the triplet and doublet fields and such mixing is proportional to the triplet VEV and thus small. The triplet fields are the main component of H^\pm, H^0, A^0 while h^0 is predominantly made up by the doublet field and act as the SM Higgs boson. For triplet Higgs bosons masses $M < 1$ TeV, the couplings h_{ij} are constrained to be $h_{ij} \leq 1$ or even much smaller than 1 by the lepton flavor violating processes such as $\mu \rightarrow e\gamma, \tau \rightarrow e(\mu)\gamma, \mu \rightarrow eee$, and $\tau \rightarrow lll$ etc[6, 8, 10, 11].

III. THE PROCESSES AND THE PARAMETERS INVOLVED

The Feynman diagrams of the LFV processes $\gamma\gamma \rightarrow \ell_i\ell_j$ ($i \neq j$ and $\ell_i = e, \mu, \tau$) induced by the charged scalars $\phi^{\pm\pm}$ and ϕ^\pm are shown in Figure 1. There are s-, t- and u- channel contributions in total with the u-channel not shown in Figure 1.

The gauge invariant amplitude of $\gamma\gamma \rightarrow \tau\bar{\mu}(\bar{e})$ induced by the scalars is given by

$$\mathcal{M} = \frac{1}{2} \bar{u}_\tau \Gamma^{\mu\nu} P_L v_\mu \epsilon_\mu(\lambda_1) \epsilon_\nu(\lambda_2) . \quad (6)$$

Explicit form of the tensor $\Gamma^{\mu\nu}$ is determined by detailed couplings which we do not shown here but has been checked many times in the program. These amplitudes contain the Passarino-Veltman one-loop functions, which are calculated by LoopTools [12].

For $\gamma\gamma$ collision, where the photon beams are generated by the backward Compton scattering of incident electron- and laser-beams just before the interaction point, through convoluting the cross section of $\gamma\gamma$ with the photon beam luminosity distribution, the events number can be written as:

$$N_{\gamma\gamma \rightarrow \ell_i\bar{\ell}_j} = \int d\sqrt{s_{\gamma\gamma}} \frac{d\mathcal{L}_{\gamma\gamma}}{d\sqrt{s_{\gamma\gamma}}} \hat{\sigma}_{\gamma\gamma \rightarrow \ell_i\bar{\ell}_j}(s_{\gamma\gamma}) \equiv \mathcal{L}_{e^+e^-} \sigma_{\gamma\gamma \rightarrow \ell_i\bar{\ell}_j}(s) , \quad (7)$$

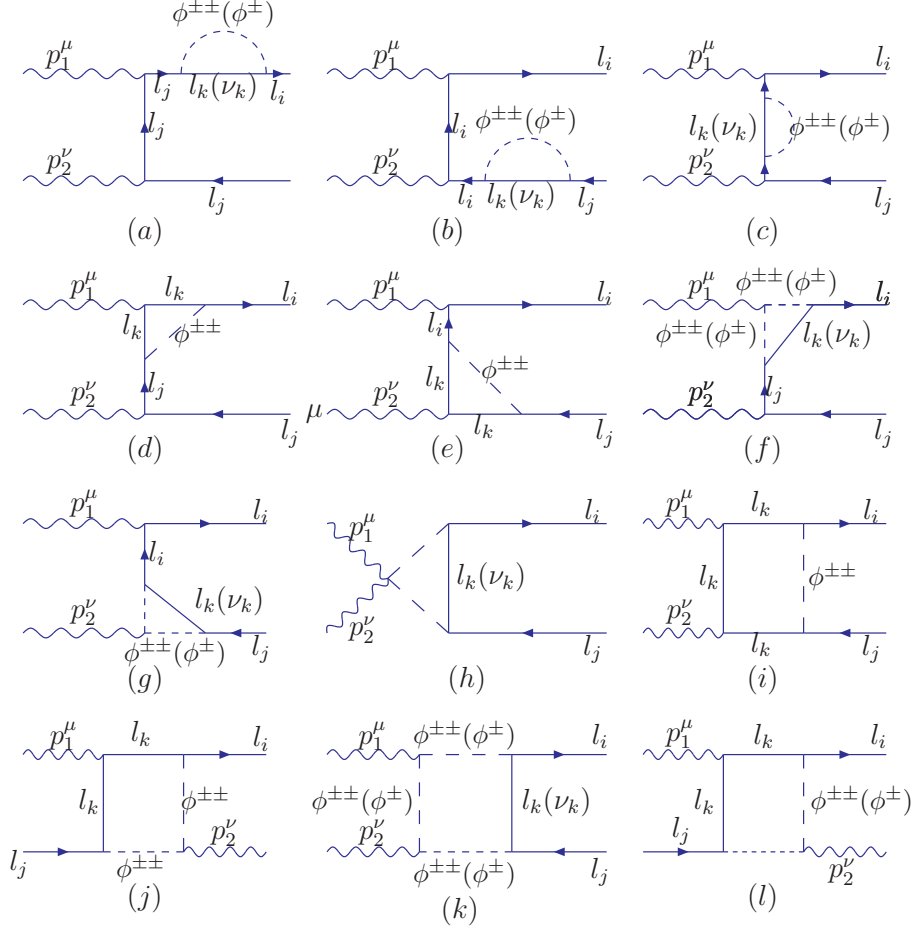


Figure 1: Feynman diagrams contributing to the process $\gamma\gamma \rightarrow \ell_i \ell_j$.

where $d\mathcal{L}_{\gamma\gamma}/d\sqrt{s_{\gamma\gamma}}$ denotes as the photon-beam luminosity distribution; $\sigma_{\gamma\gamma \rightarrow \ell_i \bar{\ell}_j}(s_{ee})$, where s_{ee} is the squared center-of-mass energy of e^+e^- collision, is the effective cross section of $\gamma\gamma \rightarrow \ell_i \bar{\ell}_j$ and in the optimum case it can be written as [13]

$$\sigma_{\gamma\gamma \rightarrow \ell_i \bar{\ell}_j}(s) = \int_{\sqrt{a}}^{x_{max}} 2z dz \hat{\sigma}_{\gamma\gamma \rightarrow \ell_i \bar{\ell}_j}(s_{\gamma\gamma} = z^2 s) \int_{z^2/x_{max}}^{x_{max}} \frac{dx}{x} F_{\gamma/e}(x) F_{\gamma/e}\left(\frac{z^2}{x}\right). \quad (8)$$

Here $F_{\gamma/e}$ is the energy spectrum of the back-scattered photon for the unpolarized initial electron and laser photon beams, which can be written as

$$F_{\gamma/e}(x) = \frac{1}{D(\xi)} \left[1 - x + \frac{1}{1-x} - \frac{4x}{\xi(1-x)} + \frac{4x^2}{\xi^2(1-x)^2} \right] \quad (9)$$

with

$$D(\xi) = \left(1 - \frac{4}{\xi} - \frac{8}{\xi^2}\right) \ln(1 + \xi) + \frac{1}{2} + \frac{8}{\xi} - \frac{1}{2(1 + \xi)^2}. \quad (10)$$

The definitions of parameters ξ and x_{max} can be found in Ref.[13] and we choose $\xi = 4.8$ and $x_{max} = 0.83$ in the numerical calculation.

As for the SM parameters involved, we take [14]

$$m_\mu = 0.106 \text{ GeV}, m_\tau = 1.777 \text{ GeV}, m_e = 0.511 \text{ MeV}, \alpha = 1/128.8, \sin^2 \theta_W = 0.223.$$

As the neutrino masses are quite small, the triplet VEV v_Δ which is responsible for neutrino masses should also be small. Small triplet VEVs are possible and could even be natural [6] by adjusting various parameters in the most general form of the Higgs potential. There are two possible realizations, firstly, authors of Ref. [15] point out that the lepton number is explicitly violated at very low energy scale M_S , which will result in a tiny v_Δ . Secondly, even if the energy scale M_S is not so tiny, i.e, $M_S \sim v$ ($v = 246 \text{ GeV}$) v_Δ can be naturally small, which is denoted as a "type II seesaw mechanism" [6]. In our work, we will choose the VEV of the triplet v_Δ at the order of the typical neutrino mass upper limit, i.e, $v_\Delta \sim 1 \text{ eV}$.

For the charged Higgs masses, the constraints are quite loose. Rough estimation can be obtained by the fact that the Higgs bosons that compose Δ will obtain masses at the electroweak scale [6, 9, 15, 16], with a neutral CP-even Higgs boson playing the role of the standard Higgs with a mass at about 125 GeV [17, 18]. So we take the masses of the scalars other than the standard Higgs boson to lie in the range of a few hundred GeV. We assume the masses degenerate unless with otherwise statement, i.e, $m_{\phi^{\pm\pm}} = m_{\phi^\pm} = m_\phi$.

Limits on the scalar mass m_ϕ can also be obtained by studying its effects on various lepton flavor violating (LFV) constraints [6, 10, 19]. It is too weak and does not conflict with the assumption that the scalar masses m_ϕ are in the order of hundred GeV. We assume that the scalar mass m_ϕ is less than 1 TeV. To investigate the dependence of the cross sections on it, three classical values: $m_\phi = 200, 500, 1000 \text{ GeV}$ are taken in our calculations.

The Maki-Nakagawa-Sakata (MNS) matrix V_{MNS} diagonalize the neutrino mass matrix mass can be written as [19, 20] :

$$V_{\text{MNS}} = \begin{pmatrix} c_{12}c_{13} & s_{12}c_{13} & s_{13}e^{-i\delta} \\ -s_{12}c_{23} - c_{12}s_{23}s_{13}e^{i\delta} & c_{12}c_{23} - s_{12}s_{23}s_{13}e^{i\delta} & s_{23}c_{13} \\ s_{12}s_{23} - c_{12}c_{23}s_{13}e^{i\delta} & -c_{12}s_{23} - s_{12}c_{23}s_{13}e^{i\delta} & c_{23}c_{13} \end{pmatrix}, \quad (11)$$

Here $s_{ij} \equiv \sin \theta_{ij}$ and $c_{ij} \equiv \cos \theta_{ij}$; δ denotes the CP-phase. For majorana neutrinos, two additional phases should be added and then the mixing matrix V is changed into

$$V = V_{\text{MNS}} \times \text{diag}(1, e^{i\phi_1/2}, e^{i\phi_2/2}), \quad (12)$$

where the discussions of the majorana phases ϕ_1 and ϕ_2 can be found in Ref. [1, 19, 21].

In the HTM the triplet Yukawa coupling h_{ij} is directly connected to the neutrino mass matrix (m_{ij}) , just as shown in Eq. (3), which is the phenomenologically attractive feature of this model. Actually, the Eq. (3) can be rewritten in the basis of the three diagonal Dirac neutrino masses by the MNS (Maki-Nakagawa-Sakata) matrix V_{MNS} [6, 20],

$$h_{ij} = \frac{m_{ij}}{\sqrt{2}v_\Delta} = \frac{1}{\sqrt{2}v_\Delta} [V_{\text{MNS}} \text{diag}(m_1, m_2 e^{i\phi_1}, m_3 e^{i\phi_2}) V_{\text{MNS}}^T]_{ij} \quad (13)$$

By expanding Eq. (13), the explicit expressions of h_{ij} can be found [6, 19, 22–24]:

$$\begin{aligned} h_{ee} &= \frac{1}{\sqrt{2}v_\Delta} \left(m_1 c_{12}^2 c_{13}^2 + m_2 s_{12}^2 c_{13}^2 e^{i\phi_1} + m_3 s_{13}^2 e^{-2i\delta} e^{i\phi_2} \right), \\ h_{e\mu} &= \frac{1}{\sqrt{2}v_\Delta} \left\{ m_1 (-s_{12} c_{23} - c_{12} s_{23} s_{13} e^{i\delta}) c_{12} c_{13} \right. \\ &\quad \left. + m_2 (c_{12} c_{23} - s_{12} s_{23} s_{13} e^{i\delta}) s_{12} c_{13} e^{i\phi_1} + m_3 s_{23} c_{13} s_{13} e^{-i\delta} e^{i\phi_2} \right\}, \\ h_{e\tau} &= \frac{1}{\sqrt{2}v_\Delta} \left\{ m_1 (s_{12} s_{23} - c_{12} c_{23} s_{13} e^{i\delta}) c_{12} c_{13} \right. \\ &\quad \left. + m_2 (-c_{12} s_{23} - s_{12} c_{23} s_{13} e^{i\delta}) s_{12} c_{13} e^{i\phi_1} + m_3 c_{23} c_{13} s_{13} e^{-i\delta} e^{i\phi_2} \right\}, \\ h_{\mu\mu} &= \frac{1}{\sqrt{2}v_\Delta} \left\{ m_1 (-s_{12} c_{23} - c_{12} s_{23} s_{13} e^{i\delta})^2 + m_2 (c_{12} c_{23} - s_{12} s_{23} s_{13} e^{i\delta})^2 e^{i\phi_1} + m_3 s_{23}^2 c_{13}^2 e^{i\phi_2} \right\}, \\ h_{\mu\tau} &= \frac{1}{\sqrt{2}v_\Delta} \left\{ m_1 (-s_{12} c_{23} - c_{12} s_{23} s_{13} e^{i\delta}) (s_{12} s_{23} - c_{12} c_{23} s_{13} e^{i\delta}) \right. \\ &\quad \left. + m_2 (c_{12} c_{23} - s_{12} s_{23} s_{13} e^{i\delta}) (-c_{12} s_{23} - s_{12} c_{23} s_{13} e^{i\delta}) e^{i\phi_1} + m_3 c_{23} s_{23} c_{13}^2 e^{i\phi_2} \right\}, \\ h_{\tau\tau} &= \frac{1}{\sqrt{2}v_\Delta} \left\{ m_1 (s_{12} s_{23} - c_{12} c_{23} s_{13} e^{i\delta})^2 + m_2 (-c_{12} s_{23} - s_{12} c_{23} s_{13} e^{i\delta})^2 e^{i\phi_1} + m_3 c_{23}^2 c_{13}^2 e^{i\phi_2} \right\}. \end{aligned} \quad (14)$$

From above equation, we can see that the couplings h_{ij} depend on the following nine parameters: the mass-squared differences Δm_{21}^2 , Δm_{31}^2 , the mass of the lightest neutrino m_0 , three mixing angles θ_{12} , θ_{13} , θ_{23} , and three complex phases (δ, ϕ_1, ϕ_2) .

Different neutrino oscillation experiments, such as the solar [25], atmospheric [26], accelerator [27], and reactor neutrinos [28], can be used to determine the mass-squared differences $(\Delta m_{21}^2, \Delta m_{31}^2)$ and the mixing angles $(\theta_{12}, \theta_{13}, \theta_{23})$. The preferred values are given in the following:

$$\begin{aligned} \Delta m_{21}^2 &\equiv m_2^2 - m_1^2 \simeq 7.9 \times 10^{-5} \text{eV}^2, \quad |\Delta m_{31}^2| \equiv |m_3^2 - m_1^2| \simeq 2.7 \times 10^{-3} \text{eV}^2, \quad (15) \\ \sin^2 2\theta_{12} &\simeq 0.86, \quad \sin^2 2\theta_{23} \simeq 1, \quad \sin^2 2\theta_{13} \simeq 0.089. \end{aligned}$$

Since the sign of Δm_{31}^2 is unknown for now, there are two neutrino mass-hierarchy patterns. One possibility is the normal hierarchy (NH), with $\Delta m_{31}^2 > 0$ where $m_1 < m_2 < m_3$ and the other is the Inverted hierarchy (IH) with $\Delta m_{31}^2 < 0$ where $m_3 < m_1 < m_2$ [6].

It is very difficult, even impossible to some extent, to extract informations on majorana phases solely from the neutrino oscillation experiments [6, 29]. Therefore, it is worthwhile to consider other possibilities, such as the LFV processes in the context of HTM, to determine the majorana phases.

As mentioned in Ref. [6, 8, 19], one can define four cases of the majorana phases as follows: Case I ($\phi_1 = 0, \phi_2 = 0$); Case II ($\phi_1 = 0, \phi_2 = \pi$); Case III ($\phi_1 = \pi, \phi_2 = 0$); Case IV ($\phi_1 = \pi, \phi_2 = \pi$). In this work we will study in detail the dependence of $\gamma\gamma \rightarrow \ell_i \bar{\ell}_j$ in each case with the new values of θ_{13} given by Daya Bay [28], i.e, $\sin^2 2\theta_{13} \simeq 0.089$.

IV. NUMERICAL RESULTS AND DISCUSSIONS

The lepton flavor changing production processes $\gamma\gamma \rightarrow \ell_i \bar{\ell}_j$, including the $e\mu$, $e\tau$ and $\mu\tau$, can be different in normal hierarchy case and inverted hierarchy case, respectively. We will discuss such two possibilities with the choices of majorana phase from case-I to case-IV.

The relevant parameters in this process include the neutrino parameters, the scalar masses and the scale parameter. The neutrino parameters are: Δm_{21}^2 , Δm_{31}^2 , m_0 , θ_{12} , θ_{13} , θ_{23} , and δ , ϕ_1 , ϕ_2 . Δm_{21}^2 , Δm_{31}^2 . The parameters θ_{12} , θ_{13} , θ_{23} , and δ take the values given by experiments in Eq. (16) and we take $\delta = 0$. Four different choices of ϕ_1 , ϕ_2 (case-I to case-IV) will be discussed in our study. The remaining m_0 , the lightest neutrino mass, is quite small. The upper limit for the summation of all the neutrino masses [30] is given by $\sum m_\nu \leq 0.28$ eV (95% *CL*) assuming a flat Λ CDM cosmology. Thus we will take the mass range of m_0 to be $0 \leq m_0 \leq 0.3$ eV as an estimation..

It has been shown that the coupling constants h_{ij} , especially h_{ee} , $h_{e\mu}$ which are the functions of the neutrino flavor parameters, should satisfy certain constraint, i.e. h_{ee} , $h_{e\mu} \sim 0$, $h_{e\tau}$, $h_{\tau\mu} < 1$ [6, 8, 10, 11, 31]. We will take into account such constraints in the results we obtained.

Finally, the charge conjugate process $\gamma\gamma \rightarrow \bar{\ell}_i \ell_j$ production channel will also be included in our numerical study.

A. Normal Hierarchy

By simple estimations from the expressions of the $h_{ij}(i, j = e, \mu, \tau)$, we can see that their values have large hierarchy. So we can discuss the productions $\gamma\gamma \rightarrow \mu\bar{e}$, $\tau\bar{e}$, and $\mu\bar{\tau}$ one by one in the four cases of ϕ_1 and ϕ_2 .

1. $\gamma\gamma \rightarrow \mu\bar{e}$

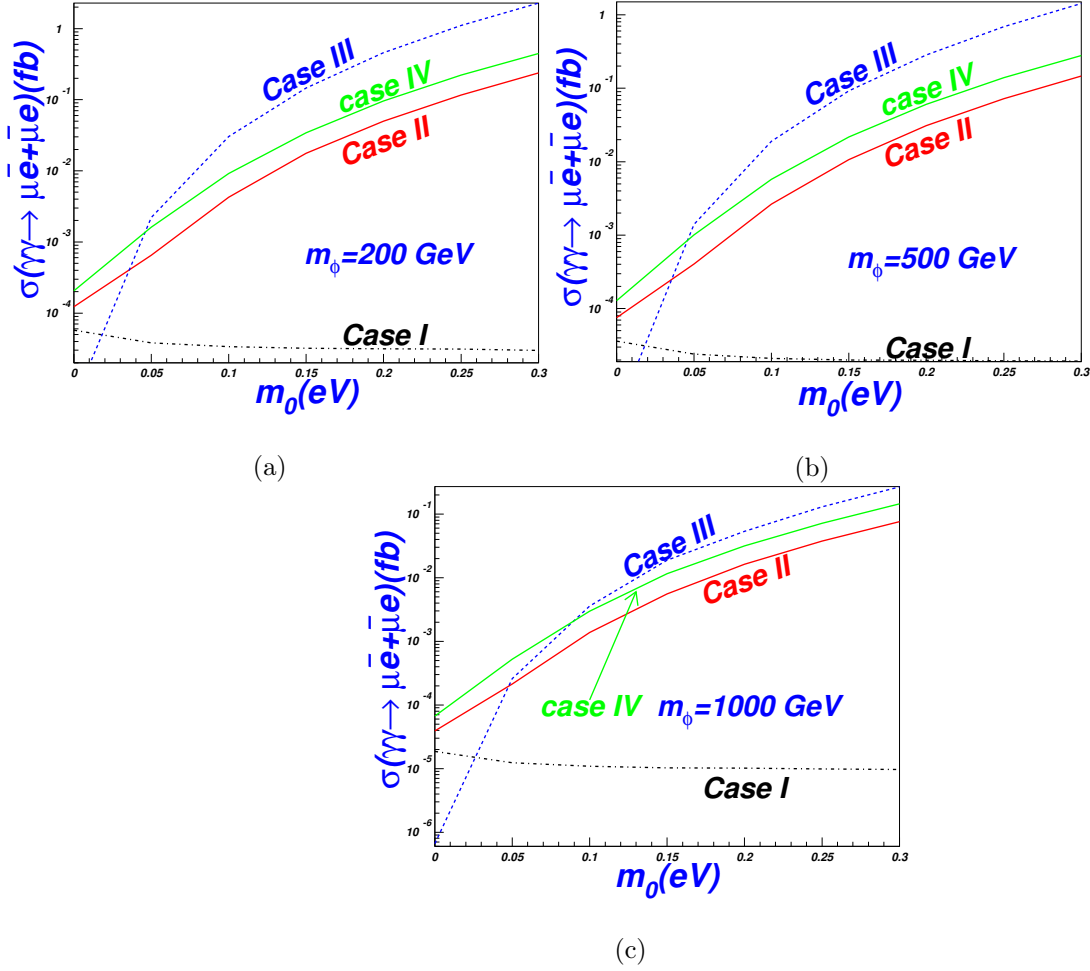


Figure 2: The cross section σ of the LFV process $\gamma\gamma \rightarrow \mu\bar{e}$ as a function of the neutrino mass m_0 for Case I to Case IV with different scalar mass: $m_\phi = 200, 500, 1000 \text{ GeV}$ for $\sqrt{s} = 500 \text{ GeV}$.

Figure 2 shows the cross sections of the $\gamma\gamma \rightarrow \mu\bar{e}$, varying with respect to the lightest neutrino mass m_0 , with different scalar mass $m_\phi = 200, 500, 1000 \text{ GeV}$. From the figure, we can see that the production rates increase with the increasing m_0 . When m_0 is small,

for example, less than 0.1 eV, the cross sections are less than 0.01 fb in most of parameter space. But when m_0 becomes large, the production rates may arrive at 2 fb in the optimum region of case III. We can also see that the cross section is also affected by the scalar mass, which may vary from 200 GeV to 1000 GeV. Such influence is however much more smaller than that from m_0 . So in the latter discussion, we will take $m_\phi = 200$ GeV.

The center-of-mass dependence of the process $\gamma\gamma \rightarrow \mu\bar{e}$ is displayed in figure 3, with $m_0 = 0.25$ eV and $m_\phi = 200$ GeV. From figure 3, we can see that the production can be much larger when the \sqrt{s} is small. For example, when $\sqrt{s} = 10$ GeV, the production rate can arrive at 260 fb in case III. But for larger center-of-mass energy, the cross sections will become small. For example, the cross section arrives at 0.55 fb when $\sqrt{s} = 500$ GeV.

In Case I, II and IV, the cross sections are a bit smaller than that of Case III. In Case I with $\phi_1 = \phi_2 = 0$, the cross section is at the order of the 10^{-3} fb and quite small. But in Case II and IV, the cross sections can arrive at tens of fb, though smaller than that of Case III.

We can see in Figure 3 that the production rates of the process $\gamma\gamma \rightarrow \mu\bar{e}$ decrease with the increasing center-of-mass energy \sqrt{s} , which is reasonable since there is no s-channel charged scalars contributions to the lepton flavor changing process and the large masses of the inner line particles may suppress the production rates further. Similar behaviors are also shown in some supersymmetric models [32, 34].

2. $\gamma\gamma \rightarrow \bar{e}\tau$ and $\gamma\gamma \rightarrow \bar{\mu}\tau$

Figure 4 and Figure 5 show the cross sections of the $\bar{e}\tau$ and $\bar{\mu}\tau$ production in the $\gamma\gamma$ collision, varying with respect to the lightest neutrino mass m_0 and center-of-mass \sqrt{s} , with the scalar mass $m_\phi = 200$ GeV for Case I, II, III and IV, respectively. We can see from them that both production rates are almost in the same order as the process $\gamma\gamma \rightarrow \mu\bar{e}$.

Figure 4 (a) and Figure 5 (a) show the m_0 dependence of the cross sections of the two processes $\gamma\gamma \rightarrow \bar{e}\tau$ and $\gamma\gamma \rightarrow \bar{\mu}\tau$. We can see that the production rates increase with the increasing neutrino mass and decline with the raising center-of-mass energy of ILC.

Figure 4 (b) and Figure 5 (b) give the center-of-mass dependence of the cross sections of the $\bar{e}\tau$ and $\bar{\mu}\tau$ production, from which we can see that the behaviors are the same as those of the process $\gamma\gamma \rightarrow \mu\bar{e}$. Their production rates become smaller with increasing center-of-mass

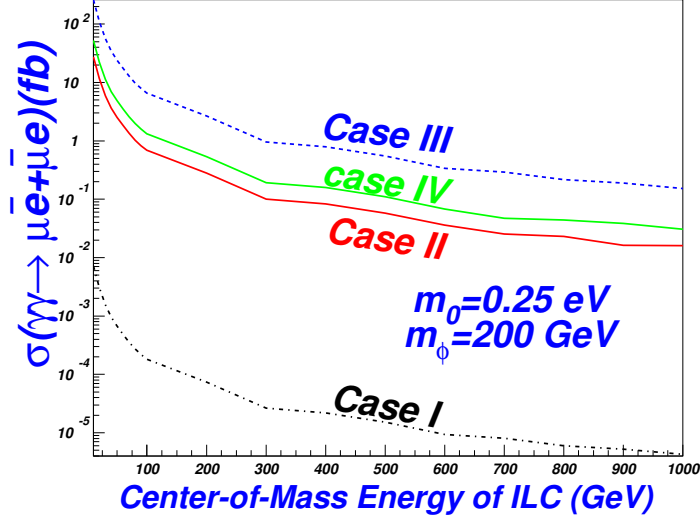


Figure 3: The cross section σ of the LFV process $\gamma\gamma \rightarrow \mu\bar{e}$ as a function of the center-of-mass \sqrt{s} for Case I to Case IV, with the scalar mass $m_\phi = 200$ GeV and the minimal neutrino mass $m_0 = 0.25$ eV.

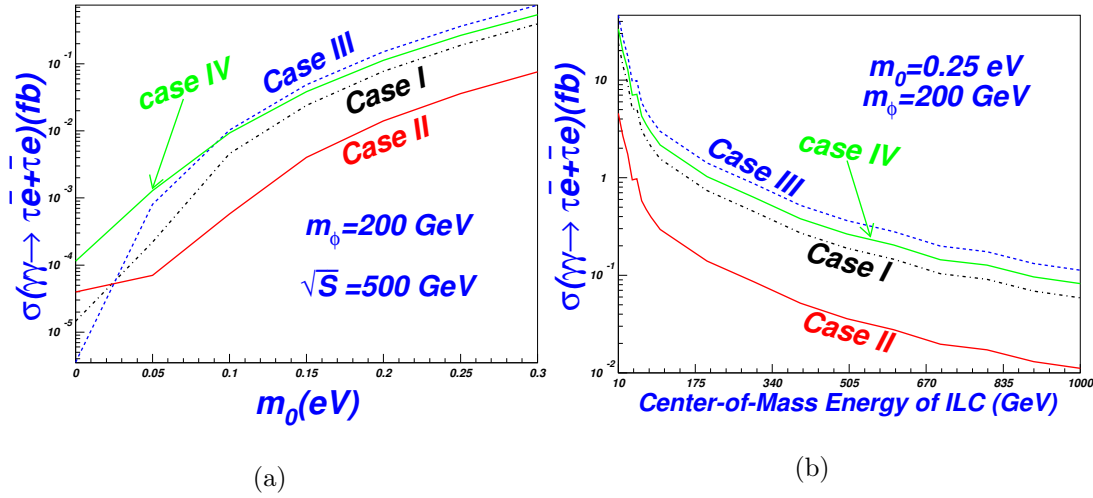


Figure 4: The cross section σ of the LFV process $\gamma\gamma \rightarrow \tau\bar{e}$ and as a function of the minimal neutrino mass m_0 (a) (for $E = 500$ GeV) and the center-of-mass energy E (b) (for $m_0 = 0.25$ eV) from Case I to Case IV, with $m_\phi = 200$ GeV.

energy of the ILC.

We have seen from Figure 2, 4, 5 that the production rates of the lepton flavor changing processes increase with increasing m_0 . This is justified since the flavor couplings are directly connected to the neutrino masses. So these processes may provide a good environment to detect the neutrino masses.

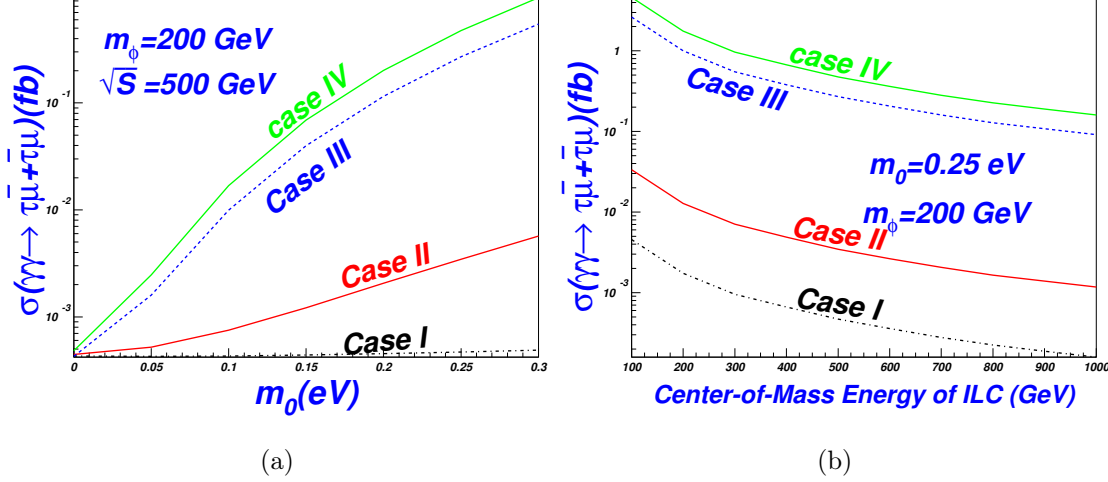


Figure 5: Same as Figure 4, but for $\gamma\gamma \rightarrow \tau\bar{\mu}$.

We can also see that the cross sections of the production processes $\bar{e}\mu$, $\bar{e}\tau$ and $\bar{\mu}\tau$ are almost in the same order with fixed center-of-mass energy of the ILC. For Case IV with $\phi = \pi$, $\phi = \pi$ and setting $m_0 = 0.25$ eV and $\sqrt{s} = 500$ GeV, the corresponding rates are 0.22 fb, 0.264 fb and 0.47 fb, respectively.

B. the Inverted Neutrino Mass Hierarchy

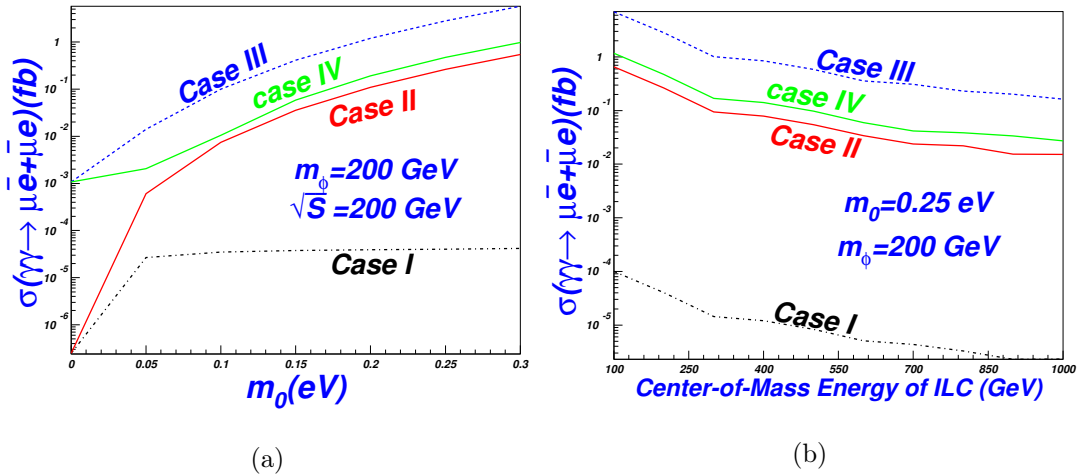


Figure 6: The LFV process $\gamma\gamma \rightarrow \mu\bar{e}$ cross section σ in the case of the Inverted Neutrino Mass Hierarchy as a function of the minimal neutrino mass m_0 and the center-of-mass energy of ILC from Case I to Case IV: with the scalar mass $m_\phi = 200$ GeV.

We also study the three productions in the inverted hierarchy case. The results can be

found in the Figures 6, 7 and 8, from which we can see that the production rates are almost the same as that in the normal hierarchy. So we will not discuss them in detail.

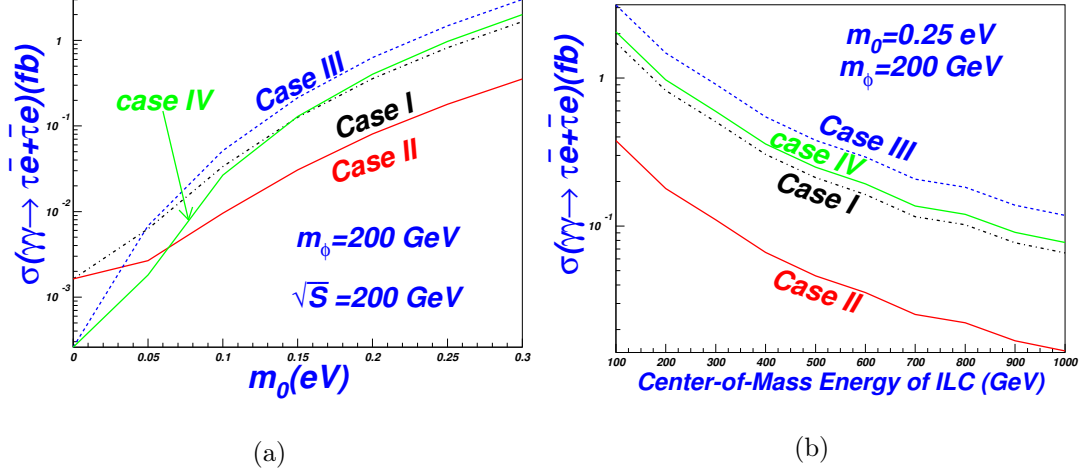


Figure 7: Same as Figure 6, but for $\gamma\gamma \rightarrow \tau\bar{\tau}$.

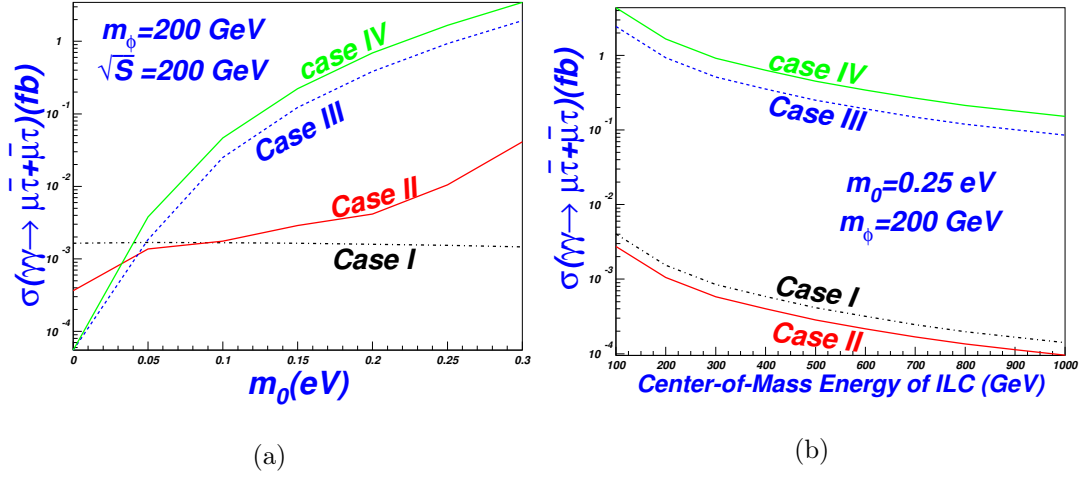


Figure 8: Same as Figure 6, but for $\gamma\gamma \rightarrow \tau\bar{\mu}$.

C. $h_{e\mu} = h_{ee} \approx 0$ constraints

After the calculations of the cross sections for each of the four cases, we turn to the constraints from the $\mu \rightarrow 3e$ and $\mu \rightarrow e\gamma$ [6, 8, 10, 11, 31] and find that the couplings $h_{e\mu}$ and h_{ee} should be quite small. We take the limit $h_{e\mu} = h_{ee} \approx 0$ to see the differences in the production rates. We will discuss how the constraint $h_{e\mu} = h_{ee} \approx 0$ can affect the production rates with $h_{e\tau}$, $h_{\mu\mu}$, $h_{\mu\tau}$, $h_{\tau\tau}$ being fixed by the assumptions in Case I to Case IV.

Figure 9 gives the cross sections of the $\gamma\gamma \rightarrow e\mu$, $e\tau$, $\mu\tau$ production rates from Case I to Case IV, from which we can see that the production rates are different from those without the constraints. To estimate the effects, we can compare the figure with Figures 2 (a), 4 (a) and Figure 5 (a). We find that the rates with the constraints $h_{e\mu} = h_{ee} \approx 0$ are about one order lower than those without the constraints. This is reasonable because the constraints $h_{e\mu} = h_{ee} \approx 0$ switch off the contributions from the Yukawa couplings $h_{e\mu}$ and h_{ee} .

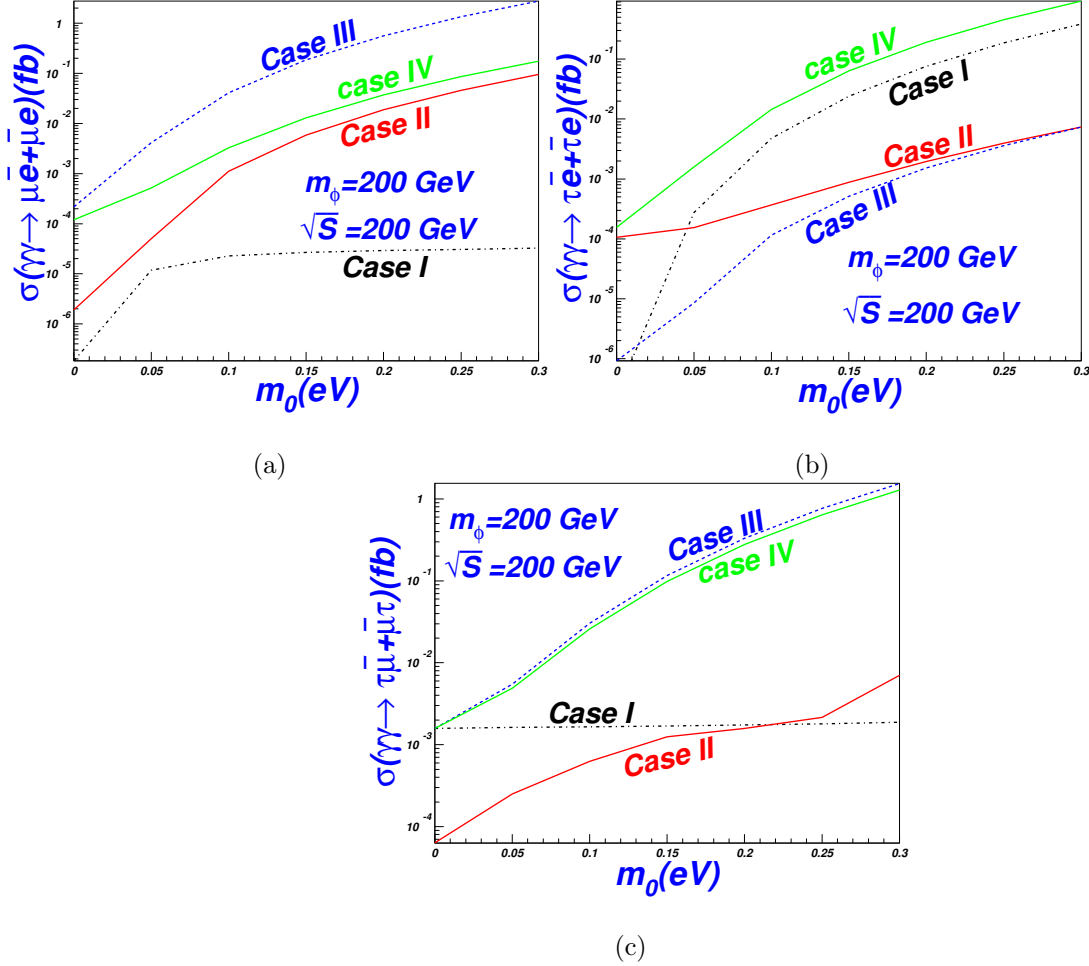


Figure 9: The cross section σ of the LFV process $\gamma\gamma \rightarrow e\mu$, $\tau\bar{e}$ and $\tau\bar{\mu}$ as a function of the neutrino mass m_0 from Case I to Case IV, for the scalar mass $m_\phi = 200$ GeV and $\sqrt{s} = 200$ GeV, with the constraints $h_{e\mu} = h_{ee} \approx 0$.

Besides, to see the results clearer, we also show the cross sections with and without LFV constraints $h_{e\mu} = h_{ee} \approx 0$ in Figure 10, from which, we can see that the production rates are suppressed by the constraints.

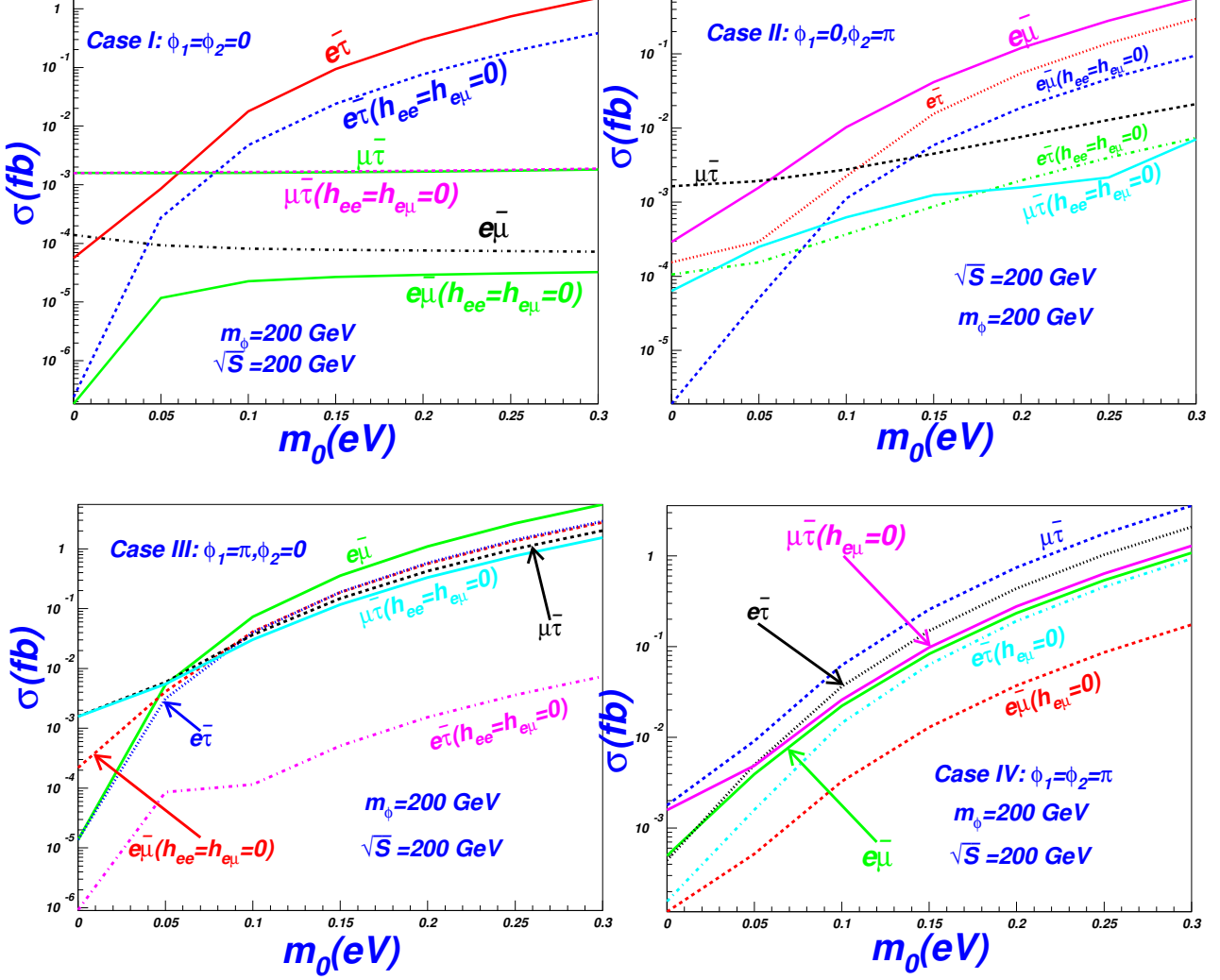


Figure 10: Same as Figure 9, but compare the results with and without the constraints $h_{e\mu} = h_{ee} \approx 0$ in the same plots.

D. Scan ϕ_1 and ϕ_2 from $-\pi$ to π

Since the ϕ_1 and ϕ_2 can affect greatly the relevant results, which can be seen from the four cases we have discussed in Figures 2, 3, 4, 5 and 9, we will scan the ϕ_1 and ϕ_2 from $-\pi$ to π and see the allowed range of ϕ_1 and ϕ_2 with the constraints $h_{e\mu} = h_{ee} \approx 0$. This can be studied in both the normal hierarchy and inverted hierarchy. We summarize the results in Table I.

From Table I, we can see that the smallest cross sections for the LFV processes are quite small, especially when m_0 is smaller than 0.1 eV and the values are less than 10^{-3} fb. From the scan, we can see that the smallest result for $\gamma\gamma \rightarrow \mu\bar{e}$ in the normal hierarchy is 0.00098

fb, but most of the cross sections are larger than 0.1 fb and can even reach 1 fb in certain regions of the parameter space. So in much of the allowed parameter space, the cross sections are large. Besides, the allowed parameter space is not small.

m_0 (eV)	Normal Hierarchy			Inverted Hierarchy		
	$\mu\bar{e}$	$\tau\bar{e}$	$\tau\bar{\mu}$	$\mu\bar{e}$	$\tau\bar{e}$	$\tau\bar{\mu}$
0.25	(0.001,6.30)	(0.0008,1.53)	(0.002,3.66)	(0.000013,1.38)	(0.0003,0.44)	(0.002,1.83)
0.15	(0,0.186)	(0.000001,0.06)	(0.00006,0.53)	(0.000004,0.20)	(0.000003,0.04)	(0.002,0.53)
0.05	(0,0.004)	(0,0.002)	(0.00002,0.014)	(0.000001,0.0056)	(0.000002,0.002)	(0.00004,0.014)
0.00	(0,0.0002)	(0,0.000)	(0,0.0017)	(0,0.0003)	(0,0.0002)	(0.00004,0.002)

Table I: Varying $-\pi < \phi_1, \phi_2 < \pi$, approximate allowed ranges of the cross sections of $\gamma\gamma \rightarrow \ell_i \ell_j$ ($i, j = e, \mu, \tau$) for several values of m_0 are shown. Other parameters are the same as in Figure 2. We take the normal and the inverted neutrino mass hierarchy and the energy of ILC at 200 GeV. The cross section are in the unit of fb and those too small are labeled as 0.

E. the SM Backgrounds of the $\gamma\gamma \rightarrow \ell_i \bar{\ell}_j$

With the following kinematical cuts [32]: $|\cos \theta_e| < 0.9$ and $p_T^e > 20$ GeV, the main SM backgrounds for the process $\gamma\gamma \rightarrow \tau\bar{e}$ are $\gamma\gamma \rightarrow \tau^+\tau^- \rightarrow \tau\nu_e\bar{\nu}_\tau\bar{e}$, $\gamma\gamma \rightarrow W^+W^- \rightarrow \tau\nu_\tau\nu_e\bar{e}$ and $\gamma\gamma \rightarrow \tau\bar{e}\nu_\tau\nu_e$ which are suppressed to be 9.7×10^{-4} fb, 1.0×10^{-1} fb and 2.4×10^{-2} fb [32], respectively. Given 3.45×10^2 fb $^{-1}$ integrated luminosity of the photon collision[33], the production rates of $\gamma\gamma \rightarrow \mu\bar{e}$, $\tau\bar{e}$, $\tau\bar{\mu}$ must be larger than 2.5×10^{-2} fb to get the 3σ observing significance [32, 34].

We see from above Figures 4 and 7 that under the current bounds that $h_{e\mu} \sim h_{ee} \sim 0$ [6, 8, 10, 11, 31] when the lightest neutrino mass is not too small, e.g, $m_0 \geq 0.1$ eV, the LFV process $\gamma\gamma \rightarrow \tau\bar{e}$ is large enough to enhance the production rate to 3σ sensitivity and may be probed in the future ILC collider.

Unlike the process $\ell_i \bar{\ell}_j$ production in supersymmetry[32, 34], the lightest Higgs with T-Parity[35] and TC2 models[36], the cross section of the $\gamma\gamma \rightarrow \mu\bar{e}$ is not definitely smaller than those of $\gamma\gamma \rightarrow \tau\bar{\mu}$, $\tau\bar{e}$, though the constraints from $\mu \rightarrow e\gamma$ and $\mu \rightarrow 3e$ give a quite small h_{ee} , $h_{e\mu}$. Because in the $e - u$ transition, even if we restrict the h_{ee} , $h_{e\mu}$ coupling to 0,

the other unsuppressed couplings $h_{\tau e}$, $h_{\tau\mu}$, $h_{\tau\tau}$ and $h_{\mu\mu}$, induced by all the three generations of the leptons which can enter the loop and contribute, could be large. Just as shown in Figure 1, the leptons ℓ_k or ν_k ($k = 1, 2, 3$) in the loop can make the couplings arbitrary unless some constraints are put on them.

For $\tau\bar{\mu}$ and $\mu\bar{e}$ production in the photon photon collision, from Figures 2, 3, and 6, we can see that their cross sections are almost the same and a bit larger than that of the τe production. The SM backgrounds of them are the same if we neglect the mass difference of the final lepton masses. So we can conclude that detection of the $\tau\mu$ and μe production may be advantageous than that of the τe .

F. Comparison of the predictions of different models

In this section, we first briefly recapitulate the sources of lepton flavor violating transitions in different models and then compare the typical magnitudes of various LFV processes in the $\gamma\gamma$ collision predicted by different models.

It is well known that in the SM the LFV transitions are absent at tree-level by the lepton number conservation. The source of such LFV transitions in the extensions of the SM is the non-diagonality of the MNS matrix. These non-diagonal elements can be large and may induce visible processes.

As the simplest extension of the SM, the HTM may naturally have LFV mediated by the Higgs bosons at tree-level. In a popular realization of HTM, the Higgs doublet is responsible for the electroweak symmetry breaking as well as generating the fermion masses while the triplet has LFV couplings whose strength are usually parameterized by h_{ij} which is shown in Eq. (14).

In the R-parity conservation MSSM [37], the neutrino masses can be obtained by introducing right-handed neutrinos and the non-diagonal elements of the mass matrix give the LFV transitions like $\ell_i \rightarrow \ell_j$, $i \neq j$, $\ell = e, \mu, \tau$ which are induced by lepton-slepton-gaugino vertex through the diagonalization matrix U_{Lij} [37] (or sneutrino mixing).

In the R-parity violating MSSM models [38], the lepton flavor changing (LFC) couplings are provided by the L -violating coupling, with L the lepton number, and the bounds of the LFC couplings λ and λ' are given in TABLE I of the Ref. [34], from which we can see the λ and λ' are constrained to be less than 10^{-2} .

In the littlest Higgs model with T-parity (LHT) [39], the interaction between the mirror lepton and the SM lepton, such as $\bar{l}_H l Z_H (A_H)$ and $\bar{\nu}_H l W_H$, can induce LFV interactions at loop level, that is, the new T-odd gauge bosons Z_H , A_H , W_H can realize the transformation between different lepton in the loop level.

One of the dynamic EWSB models, the topcolor-assisted technicolor (TC2) model[40], is quite different from the other models. To tilt the chiral condensation in the $t\bar{t}$ direction and forbid the formation of a $b\bar{b}$ condensation, a non-universal extended $U(1)$ gauge group is needed in all TC2 models. Therefore, the existence of the extra $U(1)$ gauge bosons Z' is predicted and such new particle treats the third generation quarks and leptons differently from those in the first and second generations. That is, it couples preferentially to the third generation fermions. After the mass diagonalization from the flavor eigenbasis into the mass eigenbasis, such new particle can lead to tree-level quark and lepton flavor changing couplings.

We conclude from Table II that, the $\gamma\gamma$ collision is the better channel in enhancing the magnitude for the $\ell_i \ell_j$ ($i \neq j$) associated productions at the ILC, and the models listed there give sizable cross sections. We can also see that, though the TC2 models generally predicts much larger LFV transitions than any other models, all these models can give large contributions and may be probed at the ILC. So even if we find some signal of the LFV processes, we also need to distinguish between these various new physics models.

As discussed in the former sections, motivated by the fact that any process that is forbidden or strongly suppressed in the SM constitutes a natural laboratory to search for new physics effects, the LFV processes are of particular interests for us. It turns out that they may have large cross sections, much larger than the SM ones, for certain models such as the MSSM, TC2 models and the HTM models. We can see from Table II that the HTM model predicts LFV transition rates comparable to other new physics models predictions.

V. CONCLUSION

We have performed an analysis for the scalar-induced LFV productions of $\ell_i \ell_j$ ($i \neq j$) via $\gamma\gamma$ collision at the ILC. We find that in the optimum part of the parameter space, the production rate of $\gamma\gamma \rightarrow \ell_i \ell_j$ ($i \neq j$) can reach 1 fb. This means that we may have 100 events each year for the designed luminosity of $100 \text{ fb}^{-1}/\text{year}$ at the ILC. Since the SM

	R-conversation MSSM	R-violating MSSM	TC2	LHT	HTM
$\sigma(\gamma\gamma \rightarrow \tau\bar{\mu})$	$\mathcal{O}(10^{-2})$ [32]	$\mathcal{O}(10^{-2})$ [34]	$\mathcal{O}(1)$ [36]	$\mathcal{O}(1)$ [35]	$\mathcal{O}(10^{-1})$ fb
$\sigma(\gamma\gamma \rightarrow \tau\bar{e})$	$\mathcal{O}(10^{-1})$ [32]	$\mathcal{O}(< 10^{-1})$ [34]	$\mathcal{O}(1)$ [36]	$\mathcal{O}(10^{-1})$ [35]	$\mathcal{O}(10^{-1})$ fb
$\sigma(\gamma\gamma \rightarrow \mu\bar{e})$	$\mathcal{O}(10^{-3})$ [32]	$\mathcal{O}(< 10^{-3})$ [34]	$\mathcal{O}(10^{-3})$ [36]	$\mathcal{O}(10^{-1})$ [35]	$\mathcal{O}(10^{-1})$ fb

Table II: Theoretical predictions for the $\ell_i\bar{\ell}_j$ ($i \neq j$) productions at $\gamma\gamma$ collision at the ILC. The predictions beyond SM are the optimum values. The collider energy is 500 GeV.

predictions of the production rates are completely negligible, observation of such $\ell_i\bar{\ell}_j$ events would be a possible evidence of the HTM models. Therefore, these LFV processes may serve as a sensitive probe of this kind of new physics models. Since the LFV couplings are closely related to the neutrino masses, we may obtain interesting information for the neutrino masses from them if we could see any signature of the LFV processes. At the same time, we compare the results of HTM with other new physics models and find that most predictions of these models can also be observed. So if we want to distinguish between these models through possible signals, further works are necessary.

Acknowledgments

This work was supported by the National Natural Science Foundation of China under the Grants No.11105125, 11105124 and 11205023.

-
- [1] J. Schechter and J. W. F. Valle, Phys. Rev. D **22**, 2227 (1980).
 - [2] T. P. Cheng and L. F. Li, Phys. Rev. D **22**, 2860 (1980).
 - [3] See the web: <http://www.linearcollider.org/ILC/Publications/Reference-Design-Report>.
 - [4] H. Braun et al., CLIC-NOTE-764, [CLIC Study Team Collaboration], CLIC 2008 parameters, <http://www.clic-study.org>.
 - [5] B. Badelek, et al, Int.J.Mod.Phys.A19 (2004), 5097-5186; J. Gronberg, arXiv:1203.0031; R. Nisius, arXiv:hep-ex/9811024; A. Rosca, Euro. Phys. J. C33, (2004) s1044-s1046.
 - [6] A.G. Akeroyd, Mayumi Aoki, Hiroaki Sugiyama, Phys. Rev. D79, (2009) 113010.

- [7] E. Ma, M. Raidal and U. Sarkar, Phys. Rev. Lett. **85**, 3769 (2000); E. Ma, M. Raidal and U. Sarkar, Nucl. Phys. B **615**, 313 (2001).
- [8] E. J. Chun, K. Y. Lee and S. C. Park, Phys. Lett. B **566**, 142 (2003).
- [9] A. Melfo, M. Nemevsek, F. Nesti, G. Senjanovic and Y. Zhang, Phys. Rev. D **85**, (2012) 055018.
- [10] J.A. Coarasa, A. Mendez, J. Sola, Phys. Lett. B **374**, (1996) 131.
- [11] M. Kakizaki, Y. Ogura, F. Shima, Phys. Lett. B **566**, (2003) 210.
- [12] Hahn T, Perez-Victoria T, Comput. Phys. Commun., 1999, 118: 153-165; Hahn T, Nucl. Phys. Proc. Suppl., 2004, 135: 333
- [13] Ginzburg I F, *et al.* Nucl. Instrum. Meth. A 1984, 219: 5-24.
- [14] Amsler C, *et al.*, Particle Data Group. Phys. Lett. B, 2008, 667: 1-5 and 2009 partial update for the 2010 edition.
- [15] C. A. de S. Pires, Mod.Phys.Lett. A **21**, (2006) 971.
- [16] M. Lusignoli 1 A. Masiero, M. Roncadelli, Phys. Lett. B **252**, 247 (1990).
- [17] G. Aad et al. (ATLAS Collaboration), Phys. Lett. B **716**, (2012) 1.
- [18] S. Chatrchyan et al. (CMS Collaboration), Phys. Lett. B **716**, (2012) 30.
- [19] A.G. Akeroyd, Mayumi Aoki, Hiroaki Sugiyama, Phys. Rev. D **77**, (2008) 075010.
- [20] Z. Maki, M. Nakagawa and S. Sakata, Prog. Theor. Phys. **28**, 870 (1962).
- [21] S. M. Bilenky, J. Hosek and S. T. Petcov, Phys. Lett. B **94**, 495 (1980); M. Doi, T. Kotani, H. Nishiura, K. Okuda and E. Takasugi, Phys. Lett. B **102**, 323 (1981).
- [22] J. Garayoa and T. Schwetz, JHEP **0803**, 009 (2008).
- [23] M. Kadastik, M. Raidal and L. Rebane, Phys. Rev. D **77**, 115023 (2008).
- [24] P. Fileviez Perez, T. Han, G. y. Huang, T. Li and K. Wang, Phys. Rev. D **78**, 015018 (2008).
- [25] B. T. Cleveland *et al.*, Astrophys. J. **496**, 505 (1998); W. Hampel *et al.* [GALLEX Collaboration], Phys. Lett. B **447**, 127 (1999); J. N. Abdurashitov *et al.* [SAGE Collaboration], J. Exp. Theor. Phys. **95**, 181 (2002); [Zh. Eksp. Teor. Fiz. **122**, 211 (2002)] J. Hosaka *et al.* [Super-Kamiokande Collaboration], Phys. Rev. D **73**, 112001 (2006); B. Aharmim *et al.* [SNO Collaboration], Phys. Rev. Lett. **101**, 111301 (2008); C. Arpesella *et al.* [The Borexino Collaboration], Phys. Rev. Lett. **101**, 091302 (2008)
- [26] Y. Ashie *et al.* [Super-Kamiokande Collaboration], Phys. Rev. D **71**, 112005 (2005). J.L. Raaf [Super-Kamiokande Collaboration], a talk presented 23rd International Conference on Neutrino Physics and Astrophysics (Neutrino 2008), Christchurch, New Zealand, 26-31 May 2008.

- [27] M. H. Ahn *et al.* [K2K Collaboration], Phys. Rev. D **74**, 072003 (2006); P. Adamson *et al.* [MINOS Collaboration], Phys. Rev. Lett. **101**, 131802 (2008)
- [28] Daya Bay Collaboration, Phys. Rev. Lett. **108**, (2012) 171803; Chin. Phys. C **37** (2013) 011001.
- [29] S. Pascoli, S. T. Petcov and L. Wolfenstein, Phys. Lett. B **524**, 319 (2002); V. Barger, S. L. Glashow, P. Langacker and D. Marfatia, Phys. Lett. B **540**, 247 (2002); H. Nunokawa, W. J. C. Teves and R. Zukanovich Funchal, Phys. Rev. D **66**, 093010 (2002).
- [30] S. A. Thomas, F. Abdalla, O. Lahav, Phys. Rev. Lett. **105**, (2010) 031301.
- [31] Takeshi Fukuyama (Ritsumeikan U., Kusatsu), Hiroaki Sugiyama (Ritsumeikan U., Kusatsu), Koji Tsumura (ICTP, Trieste) J. High Ener. Phys. **1003**, (2010) 044.
- [32] M. Cannoni, C. Carimalo, W. Da Silva, O. Panella, Phys. Rev. D **72**, (2005) 115004; Erratum-
ibid. D **72**, (2005) 119907.
- [33] Badelek B *et al.*, Int. J. Mod. Phys. A, 2004, 19: 5097-5186.
- [34] Cao J, Wu L, Yang J. Nucl. Phys. B, 2010, 829: 370-382; Sun Yan-Bin, Han Liang, Ma Wen-Gan, Tabbakh Farshid, Zhang Ren-You, Zhou Ya-Jin, J. High Ener. Phys. **0409**, (2004) 043, 2004.
- [35] Jin-zhong Han, Xue-lei Wang, Bing-fang Yang, Nucl. Phys. B **843**, (2011) 383.
- [36] Guo-Li Liu, Science China, **53**(2010)1-6.
- [37] F. Borzumati and A. Masiero, Phys. Rev. Lett. **57**, (1986) 961; J. Hisano, T. Moroi, K. Tobe, M. Yamaguchi, Phys. Rev. D **53**, (1996) 2442; J. Hisano and D. Nomura, Phys. Rev. D **59**, (1999) 116005.
- [38] For some early works on R-violating supersymmetry, see, e.g., C. S. Aulakh and R. N. Mohapatra, Phys. Lett. B **119**, (1982) 136; L. Hall and M. Suzuki, Nucl. Phys. B **231**, (1984) 419; J. Ellis *et al.*, Phys. Lett. B **150**, 142 (1985); G. Ross and J. Valle, Phys. Lett. B **151**, 375 (1985); S. Dawson, Nucl. Phys. B **261**, 297 (1985); R. Barbieri and A. Masiero, Nucl. Phys. B **267**, 679 (1986); H. Dreiner and G.G. Ross, Nucl. Phys. B **365**, 597 (1991); J. Butterworth and H. Dreiner, Nucl. Phys. B **397**, 3 (1993).
- [39] I. Low, J. High Ener. Phys., **0410**, 067(2004); H. C. Cheng and I. Low, J. High Ener. Phys., **0408**, (2004) 061; J. Hubisz and P. Meade, Phys. Rev. D **71**, (2005) 035016; J. Hubisz, S. J. Lee and G. Paz, J. High Ener. Phys., **0606**, (2006) 041; M. Blanke, A. J. Buras, A. Poschenrieder, Recksiegel C. Tarantino, S. Uhlig and A. Weiler, J. High Ener. Phys. **0611**, (2006) 062.
- [40] Hill C T. Phys. Lett. B, 1995, 345: 483-489; Lane K and Eichten E. Phys. Lett. B, 1995, 352:

382-387; Lane K. Phys. Lett. B, 1998, 433: 96-101; Cvetič G. Rev. Mod. Phys., 1999, 71: 513
S. Wang et al., Phys. Rev. D74, (2006) 057902.